(M = Y, Dy, Ho, Tm, Yb, Lu) which also have the Yb_3S_4-type structure at low temperatures (Patrie & Flahaut, 1967).

Fig. 8 is an image corresponding to the diffraction pattern in Fig. 7. It shows the two-dimensional modulation, with the most obvious modulation fringes in the directions indicated by arrows.

References

ANDERSSON, S. & HYDE, B. G. (1982). Z. Kristallogr. 158, 119–131.
BAKKER, M. & PLUG, C. M. (1981). J. Solid State Chem. 37, 49–57.
BÖHM, H. (1975). Acta Cryst. A31, 622–628.
BÖHM, H. (1976). Z. Kristallogr. 143, 56–66.
BOWN, M. G. & GAY, P. (1958). Z. Kristallogr. 111, 1–14.
CHEVALIER, R., LARUELLE, P. & FLAHAUT, J. (1967). Bull. Soc. Fr. Minéral. Cristallogr. pp. 564–574.
COWLEY, J. M., COHEN, J. B., SOLOMON, M. B. & WUENSCH, B. J. (1979). Editors. Modulated Structures, AIP Conf. Proc. No. 53. New York: American Institute of Physics.
DOMANGE, L., FLAHAUT, J., GUITTARD, M. & LORIERS, T. (1958). C. R. Acad. Sci. 247, 1614–1616.
FLAHAUT, T., DOMANGE, L., GUITTARD, M. & LORIERS, T. (1961). Bull. Soc. Chim. Fr. pp. 102–105.
FLAHAUT, T., DOMANGE, L., PATRIE, M. & GUITTARD, M. (1960). C. R. Acad. Sci. 251, 1517–1519.

HIGGINS, T. B., RIBBE, P. H. & NAKAJIMA, Y. (1982). Am. Mineral. 67, 76–84.
HORST, W., TAGAI, T. & KOREKAWA, M. (1981). Z. Kristallogr. 157, 233–250.
HYDE, B. G., ANDERSSON, S., BAKKER, M., PLUG, C. M. & O'KEEFFE, M. (1980). Prog. Solid State Chem. 12, 273–327.
JANNER, A. & JANSSEN, T. (1977). Phys. Rev. B, 15(2), 643–658.
JANNER, A. & JANSSEN, T. (1979). Physica Sect. A, 99, 47–76.
JANNER, A. & JANSSEN, T. (1980). Acta Cryst. A36, 408–415.
JANSSEN, T. (1979). J. Phys. C, 12, 5381–5392.
KUMAO, A., HASHIMOTO, H., NISSEN, H.-U. & ENDOH, H. (1981). Acta Cryst. A37, 229–238.
McCONNELL, J. D. C. (1978). Z. Kristallogr. 147, 45–62.
McLAREN, A. C. (1978). Chem. Soc. Spec. Period. Rep. 7, 1–30.
MAKOVICKY, E. & HYDE, B. G. (1981). Struct. Bonding (Berlin), 46, 103–170.
MORIMOTO, N., KITAMURA, M. & NAKAJIMA, Y. (1975). Proc. Jpn Acad. 51, 729–732.
MORIMOTO, N., NAKAJIMA, Y. & KITAMURA, M. (1975). Proc. Jpn Acad. 51, 725–728.
NAKAJIMA, Y. & RIBBE, P. H. (1981). Am. Mineral. 66, 142–147.
PANNETIER, G. & DEREIGNE, A. (1963). Bull Soc. Chim. Fr. pp. 1850–1854.
PATRIE, M. & FLAHAUT, J. (1967). C. R. Acad. Sci. 264, 395–398.
RIBBE, P. H. (1975). Feldspar Mineralogy. Mineral. Soc. Am. Short Course Notes, 2, R1–R52; Sm.
SMITH, J. V. (1975). Feldspar Mineralogy. Mineral. Soc. Am. Short Course Notes, 2, S1–S29.
WOLFF, P. M. DE (1974). Acta Cryst. A30, 777–785.
WOLFF, P. M. DE (1977). Acta Cryst. A33, 493–497.
WOLFF, P. M. DE (1981). Acta Cryst. A37, 625–636.
YAMAMOTO, A. (1982a). Acta Cryst. B38, 1446–1451.
YAMAMOTO, A. (1982b). Acta Cryst. B38, 1451–1456.
YAMAMOTO, A. (1982c). Acta Cryst. A38, 87–92.
YAMAMOTO, A. & NAKAZAWA, H. (1982). Acta Cryst. A38, 79–86.

Structure of U–W Oxides Investigated by Means of 1 MV High-Resolution Electron Microscopy

BY N. D. ZAKHAROV, M. A. GRIBELUK AND B. K. VAINSHTEIN

Institute of Crystallography, Academy of Sciences of the USSR, Leninsky Prospekt 59, Moscow 117333, USSR

O. N. ROZANOVA

Moscow State University, Moscow, USSR

AND K. UCHIDA AND S. HORIUCHI

National Institute for Researches in Inorganic Materials, Niihari-gun, Ibaraki, Japan

Abstract

The structure of U–W oxides with the general chemical formula UW_nO_{3n+2} has been examined by 1 MV high-resolution electron microscopy. The structure models of UW_5O_{17} and UW_4O_{14} are derived from electron microscopy images taken at the 2 Å resolution level. The structures can be regarded as slightly distorted WO_3 slabs sharing U atoms. Intergrowth of WO_3 slabs of different width has been observed. The variation in slab width gave rise to strain fields. Radiation damage due to the action of 1 MV electrons and ions has been observed.

Introduction

The point-to-point resolving power of modern high-voltage electron microscopes of better than 2 Å is high enough to resolve individual metal atoms in some inorganic compounds. Therefore, high-voltage electron microscopy is a very powerful tool for crystal structure investigation (Horiuchi, Kikuchi & Goto, 1977; Bando, Watanabe, Sekikawa, Goto & Horiuchi, 1979; Horiuchi, 1982).

In the present investigation 1 MV HRTEM has been used for crystal structure determination of U–(W,Mo) oxides forming a homologous series of compounds with the general composition $U(W,Mo)_nO_{3n+2}$ (Kovba, Rozanova & Trunov, 1977; Kovba, 1971; Mahe-Paillert, 1970). Fig. 1 schematically shows a crystal structure with $n = 2$ which has been proposed for β-UMo_2O_8 and can be regarded as consisting of distorted MoO_3 slabs separated by sheets of U atoms. The symmetry is orthorhombic, $a = 7.6$, $b = 20.1$ and $c = 4.1$ Å. The unit cell has one layer of MoO_6 octahedra along c. Mo atoms are displaced from the octahedron centres up and down, alternately, by $\Delta z = \pm 0.25$ Å making the octahedra layers puckered. Molybdenum atoms are also slightly displaced along a, as indicated by the arrows.

Experimental

The initial aim was to obtain crystals with the composition $UMoW_{13}O_{44}$ ($n = 14$). The corresponding mixture of tungsten and molybdenum trioxides and uranium dioxide ($UO_{2.02}$) was heated in a sealed silica tube for 100 h at 1273 K. Three different phases were obtained. All the crystals synthesized were too small for X-ray structure analysis.
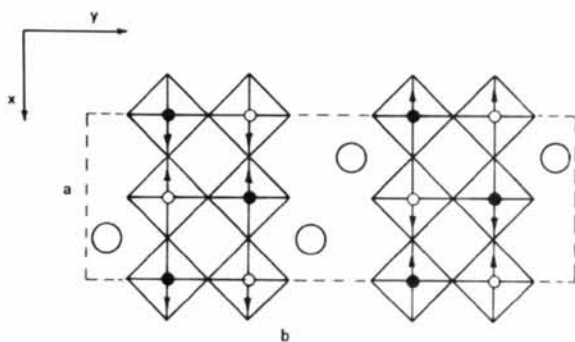
The sample was crushed in an agate mortar, dispersed in carbon tetrachloride and then collected on holey carbon film for examination in the H-1250 electron microscope operated at 1 MV accelerating voltage (Horiuchi, Kikuchi & Goto, 1977). The microscope was equipped with a biaxial goniometer stage. Usually images were taken at ×250 000 electron optical magnification. The objective aperture had a radius of 0.6 Å^{-1} in reciprocal space. The divergence of the primary electron beam was 0.8 mrad.

(a)

(b)

Fig. 1. The structure of a β-UMo_2O_8 crystal projected along c. Mo atoms are displaced up and down by $\Delta z = \pm 0.25$ Å from the sites indicated by small open and filled circles; large open circles indicate the sites of U atoms (Kovba, Rozanova & Trunov, 1977; Kovba, 1971; Mahe-Paillert, 1970).
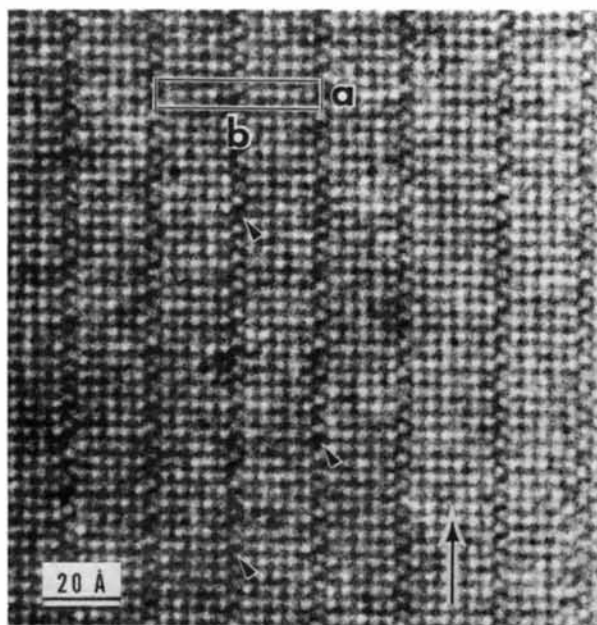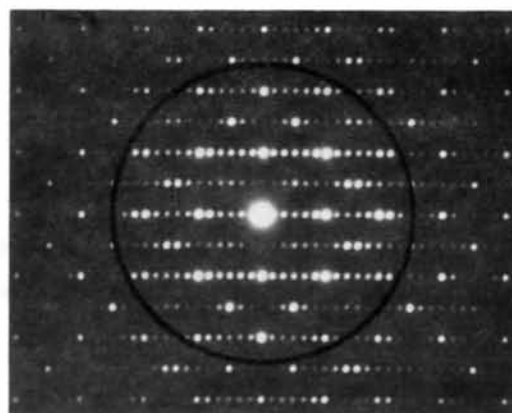
Fig. 2. (a) Image of UW_5O_{17} crystal [phase (5)] along [001] taken at overfocus $f = +500$ Å; the unit-cell dimensions are $a = 7.6$ and $b = 44.2$ Å. The arrows indicate point defects. (b) ED pattern from the crystal shown in (a); the large circle shows the size of the objective aperture used.

Electron microscopy observations

Three types of diffraction patterns were obtained from the crystal fragments under investigation. Thus, the sample prepared consisted of a mixture of at least three different phases. The first phase was a mixture of WO_3 and MoO_3 starting materials with ReO_3 structure. Some WO_3 and MoO_3 crystals were strongly reduced while the others were not.

A typical micrograph taken from a thin crystal fragment of the second phase is shown in Fig. 2(a). The picture was taken at about 500 Å overfocus so that bright dots correspond to the positions of individual metal atoms (Horiuchi, 1983). The corresponding electron diffraction pattern (Fig. 2b) has orthorhombic symmetry with unit-cell dimensions $a = 7.6$ and $b = 44.2$ Å. One can clearly see structure-fragment strips parallel to **a**, consisting of square nets of atoms which correspond to the projection of the WO_3 structure along [001]. The structure can be designated as (n), where n is the number of stacking WO_6 octahedra in each WO_3 slab along **b**. Then the structure in Fig. 2(a) may be designated as (5). Individual sites of U atoms from corrugated sheets can clearly be seen (bright dots between WO_3 slabs).

Fig. 3 shows a structure image from the third phase ($n = 4$) taken at about -300 Å underfocus; dark sites correspond to cation positions. The electron diffraction pattern inserted in Fig. 3 indicates an orthorhombic unit cell, $a = 7.6$, $b = 35.8$ Å.

Sixteen crystals had structure of type (5) and five crystals had that of type (4).

Strong preferential (001) cleavage did not permit us to observe these structures in any other orientation.

Structure model

Structural images observed gave no evidence for Mo-atom ordering. On the x–y projection U atoms are shifted by $\Delta y \simeq 0.5$ Å from the AA' line (Fig. 4a); neighbouring WO_6 octahedra are turned by several degrees with respect to one another so that two structural elements, UO_2 and WO_3, join together. Uranium atoms (Fig. 4a,b) are shifted either in the same direction or in the opposite one along **b** depending on whether n is odd or even, respectively. This is associated with different directions of WO_6 octahedra rotation. Thus, the unit cell consists, in this case, of two WO_3 slabs if n is even.

As is known, a crystal structure cannot be derived from a single projection. Yet, it is natural to suggest that in our case the crystal structure is essentially similar to that of β-UMo_2O_8 (Fig. 1). We assumed the unit cell to consist of one layer of WO_6 octahedra in the z direction ($c = 4.1$ Å). Tungsten atoms are supposed to be shifted from the centres of the octahedra by $\Delta z \simeq \pm 0.25$ Å and to form puckered layers. As a result, the unit cell is always built of two WO_3 slabs irrespective of whether n is odd or even. Taking into account the above considerations, one can derive the structure model shown schematically in Fig. 4. Crystal structure (5) belongs to the space group $Pbab$. The coordinates of W and U atoms are listed in Table 1. Experimental and calculated images show a satisfactory agreement for overfocus of approximately $+500$ Å (Fig. 5a). The crystal structure of the phase designated as (4) is, in
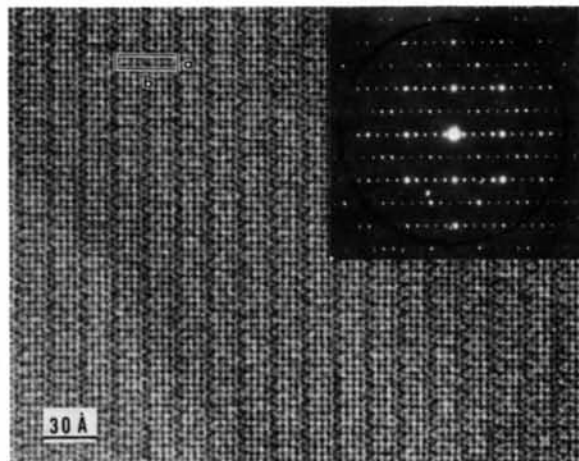

Fig. 3. The image of UW_4O_{14} [phase (4)] along [001] taken at underfocus $f = -300$ Å; the unit-cell dimensions are $a = 7.6$ and $b = 35.8$ Å.
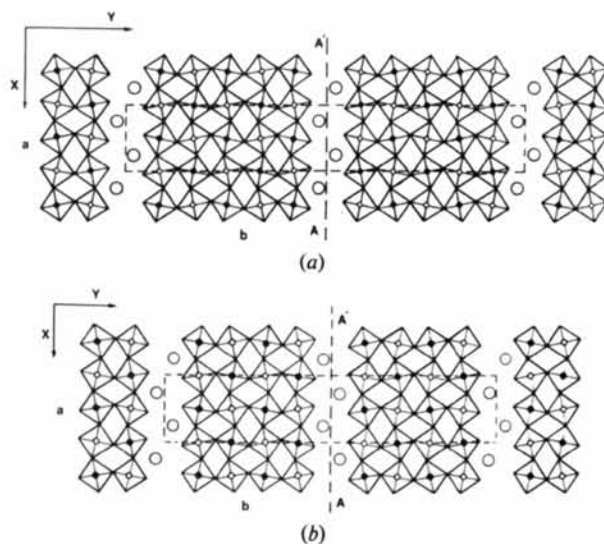

Fig. 4. The structure of (a) phase (5) and (b) phase (4) derived from EM images shown in Figs. 2 and 3. Tungsten atoms are displaced up and down and indicated by open and filled circles, respectively. Large open circles indicate U-atom positions. (a) $a = 7.6$ and $b = 44.2$ Å; (b) $a = 7.6$ and $b = 35.8$ Å

Table 1. *Atomic parameters in space group Pbab*

	x	y	z
W(1)	0·00	0·083	−0·06
W(2)	0·00	0·166	0·06
W(3)	0·00	0·250	−0·06
U(1)	0·25	0·005	0·00

Table 2. *Coordinates of metal atoms in nonequivalent positions in phase* (4), *space group Pban*

	Number of positions, Wyckoff notation and point symmetry	x	y	z
W	8 (*m*) 1	0·24	0·05	0·06
	8 (*m*) 1	0·24	0·16	0·94
U	4 (*i*) 2	0·0	0·26	0·0

principle, very similar to the previous one, differing from it in some small details. This structure (Fig. 4*b*) belongs to space group *Pban*. Coordinates of metal atoms are given in Table 2. It should be noted that the zigzag arrangement of uranium atoms means that they are 'in phase' at both sides of a WO_3 slab for even n and 'anti phase' for odd n.

Image calculation

Image calculation was carried out according to the multislice method (Cowley & Moodie, 1957; Goodman & Moodie, 1974) by means of a computer program originally developed by Skarnulis (1976) and modified by Kihlborg (1978–79). This program takes into account chromatic aberration and beam convergence (Fejes, 1977). The following parameter values were used: accelerating voltage $V = 1$ MV, spherical aberration coefficient $C_s = 10$ mm, half-angle of beam convergence 0·4 mrad, objective aperture radius $r = 0·60$ Å^{-1} and focus spread due to chromatic aberration 200 Å. The multislice procedure included 300 beams; 195 beams were selected for image formation.

Though experimental and theoretical images calculated with neutral-atom form factors were in good qualitative agreement, some quantitative differences were observed. Intensities of U-atom locations in overfocused theoretical images were brighter than the locations of W atoms, which, in fact, was not observed. A satisfactory quantitative agreement is achieved if we assume that $f_U(0)/f_W(0) \simeq 4/6$, where f_U, f_W are the atomic scattering amplitudes for U and W atoms, respectively (Fig. 5). The value of the ratio (4/6) coincides with the valence ratio for U and W atoms in our crystal. As is well known, electron microscope images are formed mainly by electrons scattered by
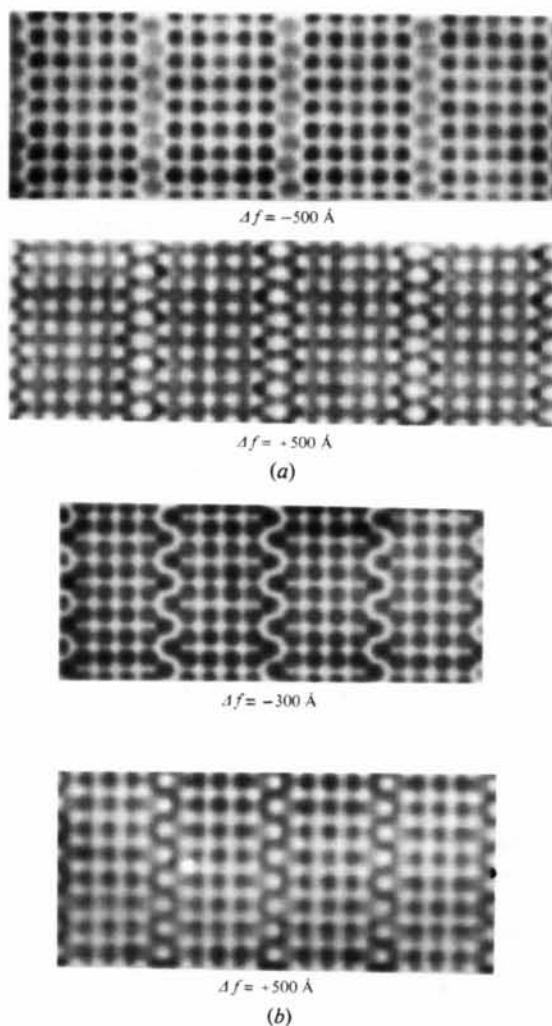

$\Delta f = -500$ Å

$\Delta f = +500$ Å

(a)

$\Delta f = -300$ Å

$\Delta f = +500$ Å

(b)

Fig. 5. Images calculated in the [001] direction for (*a*) phase (5) and (*b*) phase (4); Δf values are indicated.

outer electron shells strongly modified during bond formation. Therefore, the above assumption seems to be justified from the standpoint of the screening atomic potential (Kittel, 1963; Zakharov, Pasemann & Rozhanskii, 1982), *i.e.*

$$f(0) = 16\pi^2 \, Nme^2 \, r_s^2/(2h^2 \, \varepsilon), \qquad (1)$$

where r_s = the radius of screening which is approximately equal to half of the M–O distance (~ 1 Å), m = electron mass, e = electron charge, h = Planck's constant, N = ion charge equal to +6, +4 and −2 for W, U and O, respectively, and ε = the dielectric constant, which, in our case, is about 1 since r_s is shorter than any interatomic distance. Thus, all the above provides an interpretation of the f_U/f_W value experimentally observed.

Microsyntactic intergrowth

Microsyntactic intergrowth is often observed in the crystals under consideration. In Fig. 2 a single slab of structure (6) is present in the matrix with structure (5). Other examples of microsyntactic intergrowth are seen in the images taken at a comparatively low magnification (Figs. 6, 7). The parameter n usually ranges from 4 to 7. Such a type of crystal structure defect may be due to the inhomogeneities in the mixture of starting materials. The deviation of slab width from that for the ordered crystal results in a strain field which can often be observed by diffraction contrast (Fig. 6).
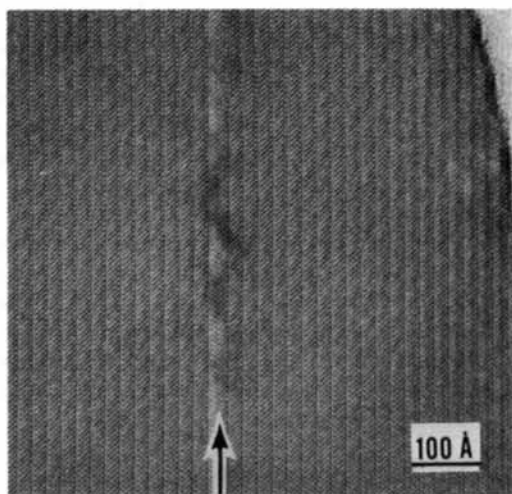

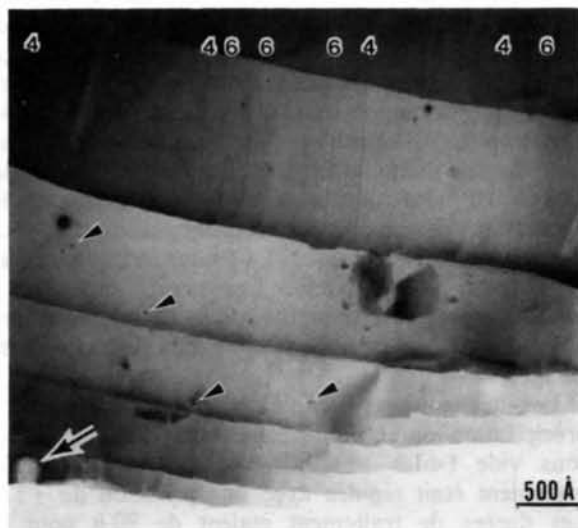Fig. 6. Single lamella with structure (7) in a (5) matrix.

Fig. 7. Image of phase (5) with lamellae of structures (4) and (6) indicated at the top. Defects which seem to be due to high-energy-ion irradiation are arrowed.
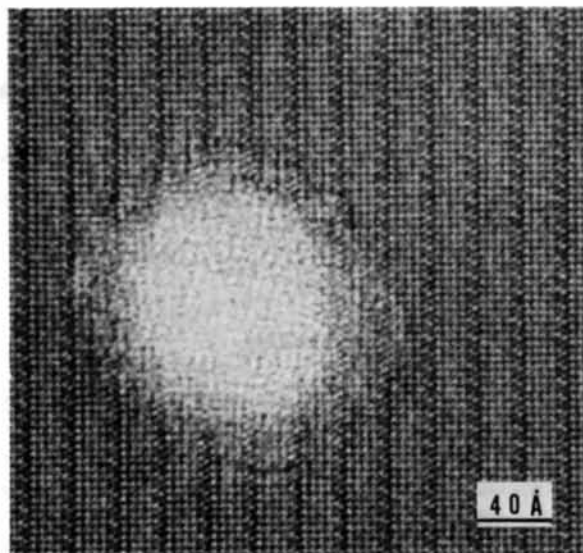

Fig. 8. A crater in UW_5O_{17} crystal which may have been formed by a high-energy ion.

Radiation damage

Fig. 2 shows that there is no contrast at some positions of U atoms, indicated by small arrows. One can explain such a contrast by the presence of U vacancies created either during the crystal formation or due to irradiation (knock-on atoms).

Figs. 7 and 8 show the craters which were also observed for such specimens. These defects are caused by high-energy ions inside the microscope.

References

BANDO, Y., WATANABE, A., SEKIKAWA, Y., GOTO, M. & HORIUCHI, S. (1979). *Acta Cryst.* A**35**, 142–145.
COWLEY, J. M. & MOODIE, A. F. (1957). *Acta Cryst.* **10**, 609–619.
FEJES, P. L. (1977). *Acta Cryst.* A**33**, 109–113.
GOODMAN, P. & MOODIE, A. F. (1974). *Acta Cryst.* A**30**, 280–290.
HORIUCHI, S. (1983). *Ultramicroscopy.* In the press.
HORIUCHI, S., KIKUCHI, T. & GOTO, M. (1977). *Acta Cryst.* A**33**, 701–703.
KIHLBORG, L. (1978–79). *Chem. Scr.* **14**, 187–196.
KITTEL, C. (1963). *Quantum Theory of Solids.* New York, London: John Wiley.
KOVBA, L. M. (1971). *Radiokhimiya,* **13**, 909–910.
KOVBA, L. M., ROZANOVA, O. N. & TRUNOV, V. K. (1977). *Radiokhimiya,* **19**, 260–264.
MAHE-PAILLERT, P. (1970). *Rev. Chim. Minér.* **7**, 807–848.
SKARNULIS, A. J. (1976). PhD Thesis, Arizona State Univ.
ZAKHAROV, N. D., PASEMANN, M. & ROZHANSKII, V. N. (1982). *Phys. Status Solidi A,* **71**, 275–281.